Segregation in the Golgi complex precedes export of endolysosomal proteins in distinct transport carriers

Yu Chen,* David C. Gershlick,* Sang Yoon Park,* and Juan S. Bonifacino

Cell Biology and Neurobiology Branch, Eunice Kennedy Shriver National Institute of Child Health and Human Development, National Institutes of Health, Bethesda, MD

Biosynthetic sorting of newly synthesized transmembrane cargos to endosomes and lysosomes is thought to occur at the TGN through recognition of sorting signals in the cytosolic tails of the cargos by adaptor proteins, leading to cargo packaging into coated vesicles destined for the endolysosomal system. Here we present evidence for a different mechanism in which two sets of endolysosomal proteins undergo early segregation to distinct domains of the Golgi complex by virtue of the proteins' luminal and transmembrane domains. Proteins in one Golgi domain exit into predominantly vesicular carriers by interaction of sorting signals with adaptor proteins, but proteins in the other domain exit into predominantly tubular carriers shared with plasma membrane proteins, independently of signal–adaptor interactions. These findings demonstrate that sorting of endolysosomal proteins begins at an earlier stage and involves mechanisms that partly differ from those described by classical models.

Introduction

The endolysosomal system of eukaryotic cells comprises an array of membrane-enclosed organelles, including early, late, and recycling endosomes, as well as lysosomes. Transmembrane proteins that reside in these compartments (hereafter referred to as endolysosomal proteins) are synthesized in the ER and subsequently transported through the cis, medial, and trans cisternae of the Golgi stack and the TGN (collectively referred to as the "Golgi complex"; Braulke and Bonifacino, 2009). The proteins are eventually delivered to the endolysosomal system either directly from the Golgi complex (Harter and Mellman, 1992; Waguri et al., 2003; Ang et al., 2004) or indirectly after transport to the plasma membrane and endocytosis (Lippincott-Schwartz and Fambrough, 1986; Braun et al., 1989; Janvier and Bonifacino, 2005). Key determinants of sorting to the endolysosomal system are signals present in the cytosolic domains of the proteins (Bonifacino and Traub, 2003), which are recognized by adaptor proteins (APs) that are components of protein coats (Robinson, 2004). Signal–adaptor interactions promote incorporation of the proteins into coated transport carriers that participate in the delivery of proteins to the endolysosomal system. Despite progress in the characterization of these molecular mechanisms, however, many aspects of endolysosomal protein sorting in the context of the whole cell remain poorly understood. These aspects include the step in the biosynthetic pathway when endolysosomal proteins diverge from plasma membrane proteins, the extent to which specific endolysosomal proteins follow the direct or indirect pathways, the nature of the transport carriers involved in either pathway, the particular signal–adaptor interactions that mediate protein incorporation into these carriers, and the possible existence of other sorting determinants. Addressing these issues in intact, living cells has proved difficult because of limitations in the ability to visualize the transport of newly synthesized endolysosomal proteins with sufficient temporal and spatial resolution and without temperature or drug manipulations that perturb the structure and function of the Golgi complex.

In this study, we have taken advantage of recent methodological developments that allow synchronization of protein transport through the biosynthetic pathway, as well as live-cell and superresolution imaging, to examine how endolysosomal proteins are sorted in the Golgi complex. Specifically, we have used the "retention using selective hooks" (RUSH) system (Boncompain et al., 2012) to track the biosynthetic transport of three transmembrane proteins with different steady-state distributions in the endolysosomal system: the cation-dependent mannose-6-phosphate receptor (CD-MPR; localized to the TGN and early/late endosomes), the transferrin receptor (TfR; plasma membrane, early endosomes, and recycling endosomes), and lysosomal-associated membrane protein (LAMP) 1 (late endosomes and lysosomes). Our analyses reveal an unexpected level of complexity in the mechanisms of endolysosomal protein sorting at the Golgi complex. We find that CD-MPR undergoes an early segregation from TfR and LAMP1 in the Golgi complex, well before their export in transport carriers.

*Y. Chen, D.C. Gershlick, and S.Y. Park contributed equally to this paper.

Correspondence to Juan S. Bonifacino: juan.bonifacino@nih.gov

Abbreviations used: AP, adaptor protein; CD-MPR, cation-dependent mannose-6-phosphate receptor; KO, knockout; LAMP, lysosomal-associated membrane protein; RUSH, retention using selective hooks; SBP, streptavidin-binding peptide; Tf, transferrin; TfR, Tf receptor; TIRF, total internal reflection fluorescence; VSV-G, vesicular stomatitis virus glycoprotein.

The Rockefeller University Press
J. Cell Biol. Vol. 216 No. 12 4141–4151
https://doi.org/10.1083/jcb.201707172

This segregation is independent of signals in the cytosolic tails but dependent on the transmembrane and luminal domains of the proteins. The CD-MPR subsequently leaves the Golgi in a population of predominantly vesicular transport carriers in a manner dependent on a cytosolic dileucine-based signal that interacts with clathrin-associated GGA adaptors. These carriers do not translocate toward the plasma membrane but directly deliver the CD-MPR to endosomes. The TfR and LAMP1, on the other hand, are exported in a population of predominantly tubular carriers destined for the plasma membrane, independently of cytosolic sorting signals and their cognate adaptors. The sorting signals in TfR and LAMP1 and the clathrin-associated AP-2 complex are, however, required for endocytosis of TfR and LAMP1 as a requisite for their eventual delivery to endosomes and lysosomes, respectively. These findings demonstrate that early segregation of different sets of endolysosomal proteins in the Golgi complex precedes their export in two distinct populations of transport carriers involved in the direct and indirect pathways. Our study also highlights distinct requirements for signal–adaptor interactions in the exit of different endolysosomal proteins from the Golgi complex.

Results

Newly synthesized endolysosomal proteins exit the Golgi complex in two distinct sets of transport carriers

Transport of newly synthesized TfR, LAMP1, and CD-MPR through the biosynthetic pathway was analyzed using the RUSH system (Boncompain et al., 2012). The endolysosomal proteins (i.e., "reporter" proteins) were genetically fused to a streptavidin-binding peptide (SBP) and a fluorescent protein (GFP or mCherry) and coexpressed with streptavidin fused to the ER-retrieval signal KDEL (Munro and Pelham, 1987; i.e., "hook" protein; Fig. 1 a). For simplicity, the reporter proteins will hereafter be referred to as TfR, LAMP1, and CD-MPR, with the implicit understanding that they are modified for use in the RUSH system. As expected, coexpression of the reporter proteins with the hook proteins resulted in their accumulation in the ER (Fig. 1 b, 0 min). Addition of the vitamin biotin competed off the SBP–streptavidin interaction, resulting in synchronous release of the proteins from the ER (Fig. 1 b and Video 1), and their eventual transport to their corresponding locations in the endolysosomal system (Fig. S1 a). Coexpression of combinations of the reporter proteins showed that they all exited the ER in the same transport carriers (Fig. S1 b) and arrived simultaneously in the Golgi complex at 15–25 min after the addition of biotin (Fig. 1, b and c). At 20–35 min, the proteins began to exit the Golgi complex in pleiomorphic transport carriers similar to those previously shown to mediate various post-Golgi transport events (Hirschberg et al., 1998; Polishchuk et al., 2000, 2003, 2006; Puertollano et al., 2003). Interestingly, we noticed the existence of two distinct populations of carriers: predominantly tubular carriers containing both TfR and LAMP1 but not CD-MPR (Fig. 2, a, b, d, and e; and Video 2), and predominantly vesicular carriers containing CD-MPR but not TfR (Fig. 2 c and Video 3; best observed with higher time resolution in Video 4). For simplicity, we refer to these carriers as "tubular" and "vesicular," respectively, notwithstanding that they display substantial variation in shape and size. Further analyses of the tubular carriers showed that they were enriched in the vesicular stomatitis virus glycoprotein (VSV-G; Fig. 2 f), a marker of transport carriers destined for the plasma membrane (Hirschberg et al., 1998; Polishchuk et al., 2006; Micaroni et al., 2013). In contrast, they were devoid of internalized transferrin (Tf; Fig. S2, a and b), indicating that they were not derived from recycling endosomes. In addition, total internal reflection fluorescence (TIRF) microscopy showed direct fusion of carriers containing TfR (Fig. S3 a and Video 5) but not internalized Tf (Fig. S3 b and Video 6), with the plasma membrane. Together, these observations indicated that TfR/LAMP1 tubular carriers bud from the Golgi and directly fuse to the plasma membrane without passing through recycling endosomes.

Early segregation of endolysosomal proteins in the Golgi complex

Airyscan superresolution imaging of cells fixed 30 min after the addition of biotin confirmed the presence of TfR and LAMP1 in tubules budding from the Golgi complex (Fig. 3, a and b) and CD-MPR in a distinct population of vesicles (Fig. 3, d and e). Surprisingly, whereas TfR and LAMP1 colocalized throughout the entire Golgi structure (Fig. 3, a and c; Pearson's coefficient = 0.95, similar to that of the same reporter protein tagged with different fluorescent proteins; Fig. S4, a and b), TfR and CD-MPR were largely segregated to different Golgi domains (Pearson's coefficient = 0.37; Fig. 3, d and f). Live-cell Airyscan imaging after the addition of biotin showed that TfR and LAMP1 continuously colocalized from their entry into the Golgi complex to their exit in tubular carriers (Fig. 3, g and i; and Video 7). In contrast, TfR and CD-MPR started to segregate shortly after their entry into the Golgi complex, and their segregation increased over time (Fig. 3, h and i; and Video 8). Similar Golgi segregation and budding patterns were observed in a different cell line, U2OS (Fig. S4, c and d). These observations thus revealed that segregation of the CD-MPR from other endolysosomal proteins begins in the Golgi complex, before their incorporation into distinct transport carriers. The sorting receptor sortilin behaved similarly to the CD-MPR (Fig. S4, e and f), demonstrating that it belongs to the same subset of endolysosomal cargos as the CD-MPR.

Exit of LAMP1 and TfR in tubular carriers is independent of signal–adaptor interactions

Sorting of TfR and LAMP1 to endosomes and lysosomes, respectively, is dependent on sorting signals fitting the YXXØ motif (where X is any amino acid and Ø a bulky hydrophobic amino acid) in the cytosolic tail of the proteins (Traub and Bonifacino, 2013; Fig. 4 a). In the case of TfR, an additional signal comprising the sequence GDNS (Fig. 4 a) contributes to sorting to the basolateral plasma membrane in polarized epithelial cells (Odorizzi and Trowbridge, 1997). Strikingly, mutation of the YXXØ and GDNS signals in TfR (residues Y20, G31, D32, N33, and S34 to alanines) and the YXXØ signal in LAMP1 (residue Y404 to alanine; Fig. 4 a) did not prevent incorporation of these proteins into the Golgi-derived tubular carriers, although it resulted in subsequent accumulation of the proteins at the plasma membrane (Fig. 4, b and c; and Video 9). YXXØ motifs are recognized by the AP complexes AP-1, AP-2, AP-3, and AP-4 (Fig. 5 a; Traub and Bonifacino, 2013) and the GDNS motif by AP-1 (Gravotta et al., 2012). CRISPR/Cas9 knockout (KO) of subunits of these complexes (Fig. 5 b) had no effect on exit of TfR and LAMP1

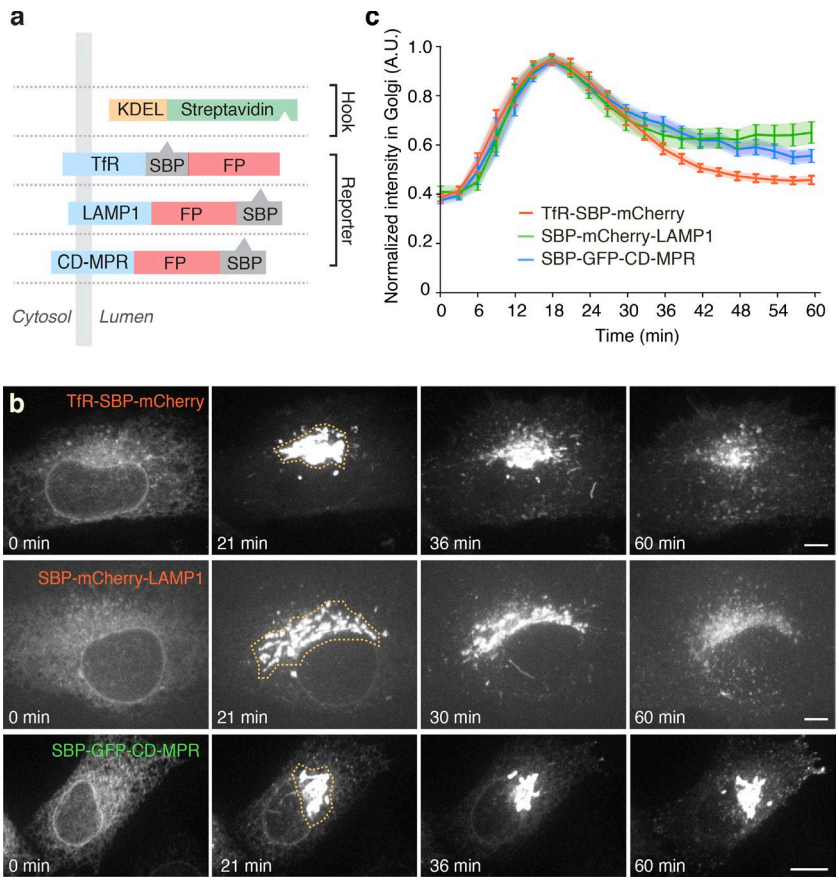

Figure 1. **Structure, localization, and ER exit of RUSH reporter proteins.** (a) Schematic representation of streptavidin–KDEL "hook" and TfR, LAMP1, and CD-MPR "reporter" proteins used in the RUSH experiments. FP, fluorescent protein (GFP or mCherry). In all figures, green and red lettering corresponds to constructs tagged with GFP and mCherry, respectively. (b) RUSH imaging series of three reporter cargos, TfR, LAMP1, and CD-MPR, expressed in HeLa cells, from Video 1. Before the addition of biotin (time 0), the three cargos exhibit a typical ER localization. At 21 min after biotin addition, the cargos localize to the Golgi. At later times, they exit the Golgi, reaching their final destination after 60 min. Bars, 5 µm. (c) Kinetics of trafficking of RUSH cargos through the Golgi complex. The normalized intensity of the masked perinuclear region indicated in b was measured across the whole time course and plotted as a function of time. Values are mean ± SEM; n = 12 cells for each cargo. Notice that the three reporter proteins released from the ER are transported into the Golgi complex at about the same time.

from the Golgi complex in tubular carriers (Fig. 5 c). KO of the AP-2 µ2 subunit, however, caused accumulation of TfR and LAMP1 at the plasma membrane (Fig. 5 d and Fig. S5, a–c), as previously shown by siRNA knockdown (Motley et al., 2003; Janvier and Bonifacino, 2005). KO of subunits of the other complexes did not prevent transport of LAMP1 to lysosomes (Fig. 5 d). These experiments indicated that interactions of cytosolic sorting signals with AP complexes are dispensable for export of TfR and LAMP1 from the Golgi complex in tubular carriers, but an interaction with AP-2 is subsequently required for endocytic delivery of the proteins to endosomes and lysosomes.

Exit of CD-MPR in vesicular carriers depends on interaction of sorting signals with GGA proteins

In contrast to TfR and LAMP1, CD-MPR has been shown to exit the Golgi by virtue of the interaction of a DXXLL motif in the cytosolic tail of the receptor (Fig. 4 a) with the monomeric clathrin adaptors GGA1, GGA2, and GGA3 (Puertollano et al., 2001, 2003; Zhu et al., 2001). Indeed, we observed that CD-MPR-containing vesicles budding from the Golgi were decorated with GGA1 (Fig. 4 d). Moreover, mutation of the DXXLL signal (residues L274 and L275 to alanine; Fig. 4 a) prevented exit of CD-MPR in the GGA1-coated carriers (Fig. 4 e). Hence, unlike Golgi export of TfR and LAMP1 in tubular carriers, export of CD-MPR in vesicular carriers depends on a specific signal–adaptor interaction. It is worth noting that the DXXLL mutant of the CD-MPR was not diverted to tubules by default but was retained in the Golgi complex. We also observed that mutation of the cytosolic sorting signals in both the TfR and CD-MPR did not prevent their segregation into different Golgi subdomains (Fig. 4 f), indicating that this phenomenon is independent of interactions with APs.

Transmembrane and luminal domains determine segregation of endolysosomal proteins in the Golgi complex

What then are the determinants of segregation in the Golgi complex and exit into tubules? To address this question, we constructed chimeric proteins having different combinations of the luminal, transmembrane, and cytosolic domains of LAMP1 and CD-MPR (both type I transmembrane proteins; Fig. 6 a) and compared their transport with that of the TfR (a type II transmembrane protein) using the RUSH system (Fig. 6, b–h). We observed that LAMP1 chimeras having the transmembrane and/or luminal domains of the CD-MPR (termed MML, LML, and MLL) were not incorporated into Golgi-derived tubules (Fig. 6 b) and were segregated from the TfR in the Golgi complex (Fig. 6, e, g, and h). In contrast, a chimera having the transmembrane and luminal domains of LAMP1 and the cytosolic tail of CD-MPR (LLM) was exported into tubules (Fig. 6 b) and colocalized with TfR in the Golgi complex (Fig. 6 f). These results indicated that transmembrane and/or luminal domains determine protein segregation within the Golgi complex that precedes exit into distinct transport carriers.

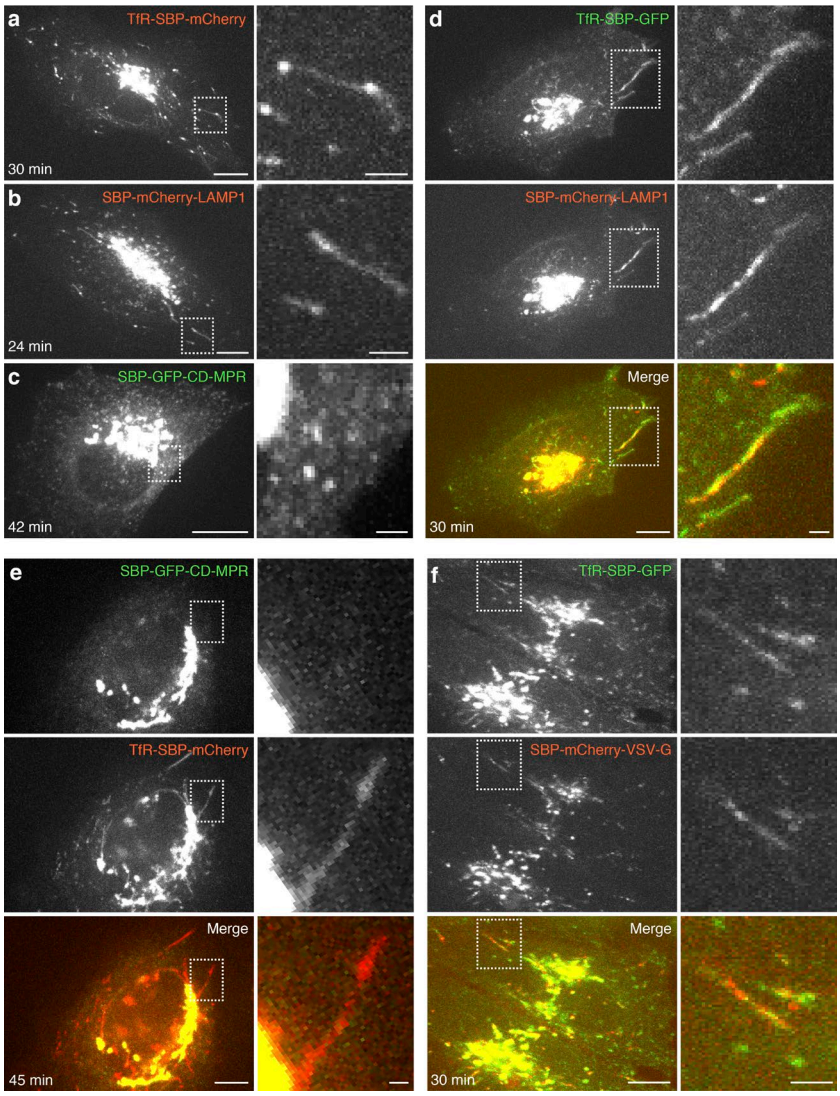

Figure 2. **Endolysosomal proteins are exported from the Golgi complex in two distinct populations of transport carriers.** (a–c) HeLa cells coexpressing streptavidin–KDEL with each of the indicated reporter proteins were treated with biotin and imaged live by spinning-disk confocal microscopy. The left panel shows single frames captured at the indicated times after addition of biotin. The right panel shows magnified images of the boxed areas. (d–f) HeLa cells coexpressing streptavidin–KDEL with combinations of the indicated reporter constructs were analyzed as in a–c. The left columns show single frames captured at the indicated times after addition of biotin (from Video 2 in d and Video 3 in e). The right columns show magnified images of the boxed areas. Bars: (low magnification) 5 µm; (high magnification) 1 µm.

Discussion

Cargo segregation in the early Golgi complex

The TGN has been classically regarded as the Golgi subcompartment where newly synthesized proteins destined for secretory vesicles, the plasma membrane, endosomes, and lysosomes are sorted into distinct populations of transport carriers (Griffiths and Simons, 1986). In this classical view, all cargo proteins remain mixed throughout the Golgi complex until they are packaged into their corresponding transport carriers. Several findings, however, challenge the notion that all cargo sorting in the Golgi complex occurs at the TGN. First, transmembrane cargos were shown to partition from Golgi enzymes during their transport through the Golgi cisternae (Patterson et al., 2008). In addition, the contents of different types of secretory granule were found to segregate from one another as early as in the cis-Golgi cisternae (Clermont et al., 1992). Other studies showed that proteoglycans aimed for the apical or basolateral surfaces of polarized epithelial cells acquire different carbohydrate modifications in the Golgi complex (Tveit et al., 2005; Vuong et al., 2006), and high-mannose forms of basolateral and apical proteins exhibit different detergent solubility, all suggestive of s egregation in the early Golgi complex (Alfalah et al., 2005). Using superresolution and live-cell imaging, we now provide direct evidence that two sets of transmembrane proteins destined for the endolysosomal system undergo progressive segregation into distinct Golgi domains before their export into distinct transport carriers. These findings indicate that cargo sorting can occur early in the Golgi complex, even for proteins that are targeted to the same organellar system. The Golgi domains to which proteins are segregated could correspond to the center or the rims of the same cisternae or to different cisternae. They could also be discrete ministacks laterally connected as part of a larger Golgi ribbon (Yano et al., 2005; Puthenveedu et al., 2006). Ultrastructural methods in combination with the RUSH system will be required to determine the exact identity of these domains.

Early segregation determines export from different Golgi sites

Early segregation likely determines the sites of cargo export from the Golgi complex. For proteins that require interaction with clathrin adaptors (e.g., CD-MPR, sortilin; Nielsen et al., 2001; Puertollano et al., 2001; Zhu et al., 2001), the early segregation domain must be connected to the TGN, which is where

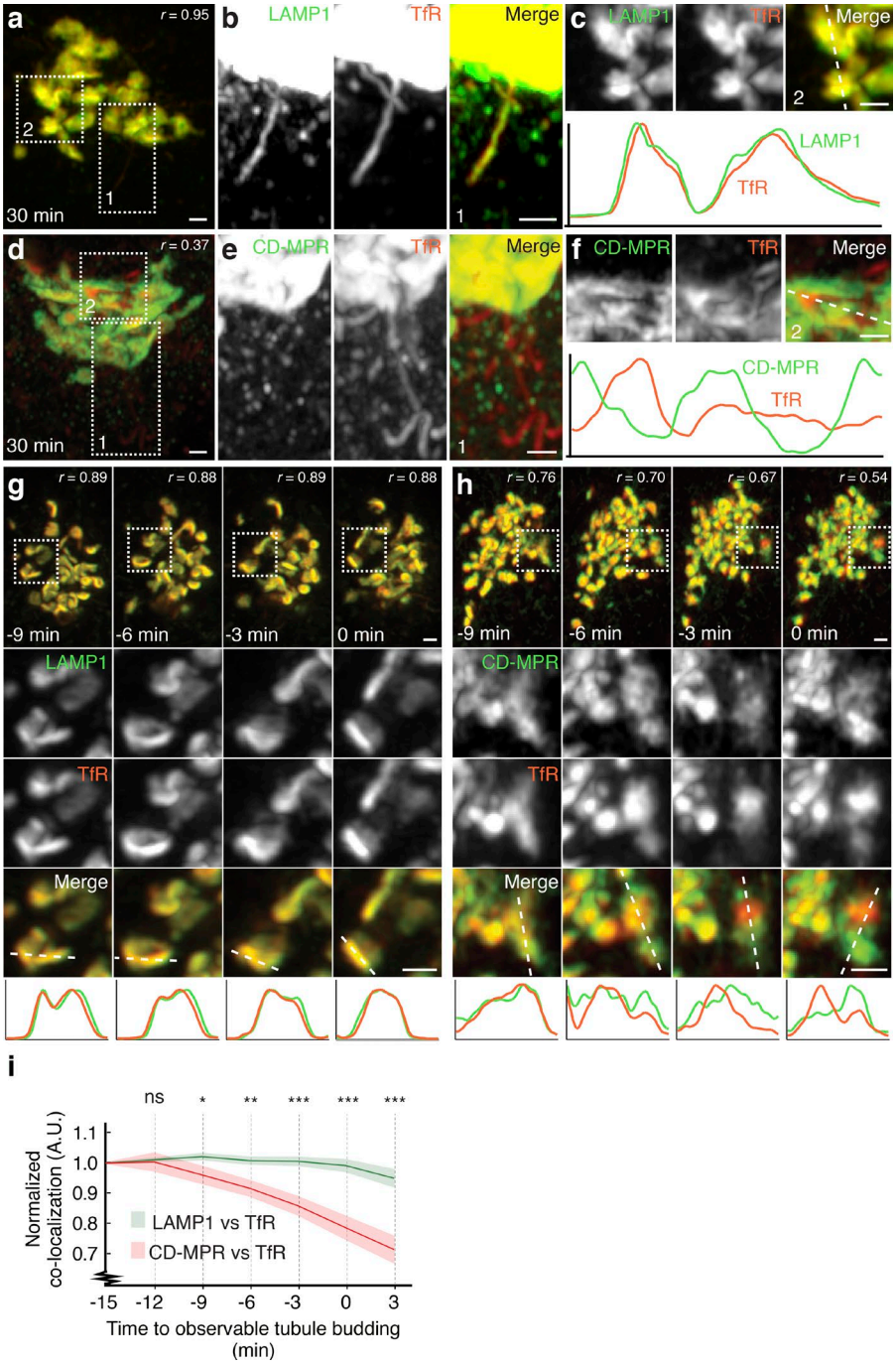

Figure 3. **Segregation of endolysosomal proteins in the Golgi complex.** (a–f) HeLa cells coexpressing streptavidin–KDEL with combinations of the indicated reporter proteins were fixed 30 min after the addition of biotin and imaged by Airyscan microscopy. (a and d) Golgi complexes of representative cells. (b and e) Magnified views of box 1. (c and f) Magnified views of box 2 and plots of fluorescence intensity along the white dashed lines. (g and h) HeLa cells coexpressing streptavidin–KDEL with combinations of the indicated reporter proteins were imaged live by Airyscan microscopy. The top rows show Golgi complexes from representative cells. The middle rows show magnifications of the boxed region. The bottom row shows plots of fluorescence intensity along the white dashed lines. Bars, 1 µm. (i) Pearson's coefficients (*r*) of data sets of which g and h are representative. Values were normalized to 1.0 at the first time point and are represented as mean ± SEM ($n = 7$ cells for each pair of cargos). ns, not significant; *, $P < 0.1$; **, $P < 0.01$; ***, $P < 0.001$. Times indicated in g–i are normalized to observable initiation of tubule budding, allowing comparative statistics.

clathrin coats are located in the Golgi complex (Klumperman et al., 1993). Proteins that exit independently of clathrin adaptors (e.g., TfR, LAMP1, and plasma membrane proteins; Pols et al., 2013), on the other hand, could be exported from a nonclathrin TGN domain or an earlier cisterna. In support of this latter possibility, electron tomography studies showed the presence of a still unidentified nonclathrin, "lace-like" coat at the rims of Golgi cisternae proximal to, but distinct from, the TGN (Ladinsky et al., 1994). These sites were proposed to mediate protein export to the plasma membrane (Ladinsky et al., 1994), although evidence for this function remains to be obtained. Furthermore, fluorescence microscopy of nocodazole-fragmented Golgi ministacks suggested that plasma membrane–directed cargos such as VSV-G exit from the Golgi stack before reaching the TGN (Tie et al., 2016). Thus, early cargo segregation in the Golgi stack likely determines export from different Golgi subcompartments.

Export of endolysosomal proteins in distinct transport carriers

Our studies also show that endolysosomal proteins leave the Golgi complex in two types of transport carrier. Both types have variable sizes and shapes, although they tend to be predominantly tubular or vesicular in appearance. The characteristics of these carriers likely reflect the Golgi compartments from which they arise. The carriers containing TfR and LAMP1 probably correspond to the VSV-G Golgi–to–plasma membrane carriers previously characterized by correlative light-electron

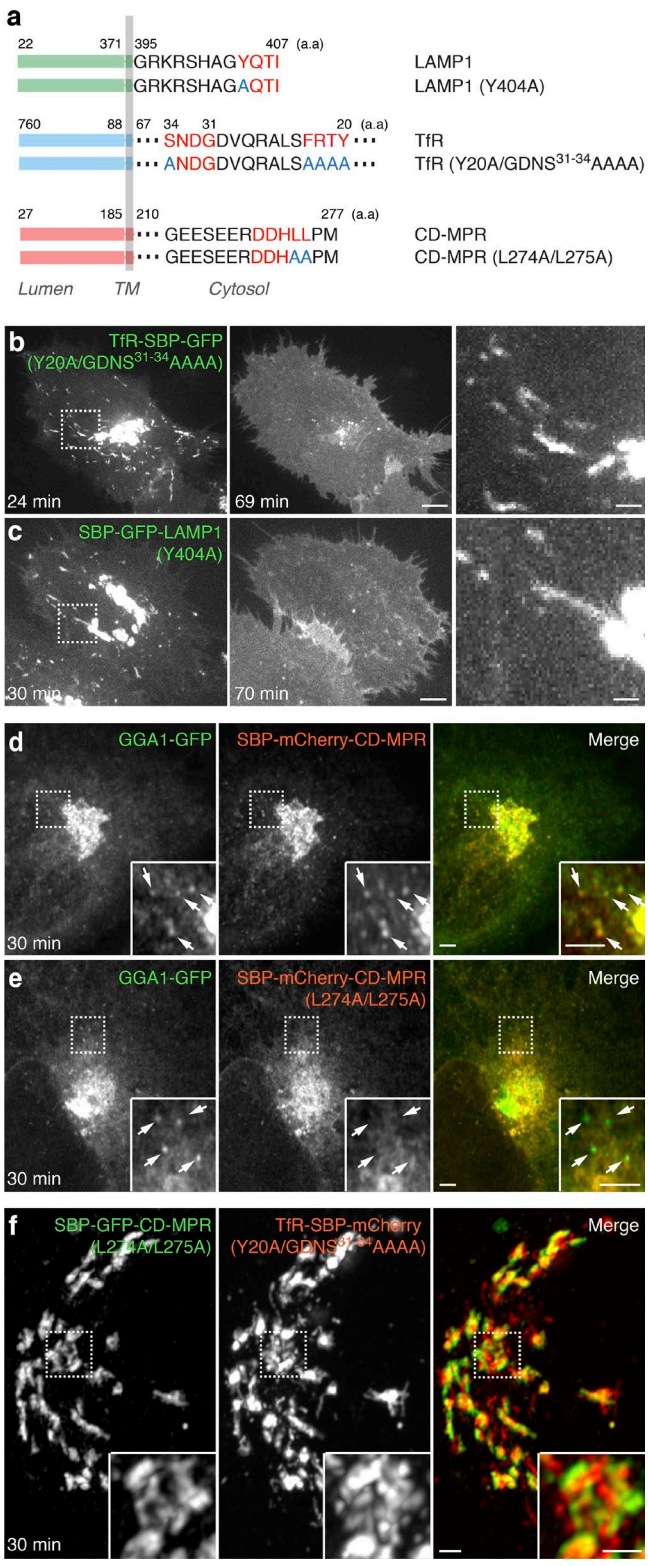

Figure 4. **Role of adaptor-binding motifs in export and segregation of endolysosomal proteins at the Golgi complex.** (a) Sequences from the cytosolic domains of TfR, LAMP1, and CD-MPR. Motifs that bind to AP complexes in each protein are highlighted in red. Mutations are indicated with blue letters. (b and c) HeLa cells coexpressing streptavidin–KDEL together with TfR and LAMP1 reporter constructs having mutations in AP-binding motifs, namely TfR-Y20A/GDNS$^{31\text{-}34}$AAAA (b) or LAMP1-Y404A (c), were imaged live by spinning-disk confocal microscopy. Images are single frames from Video 9. The times after addition of biotin are indicated. (Right) Magnifications of the boxed regions. Bars: (low magnification) 5 µm; (high magnification) 1 µm. (d and e) HeLa cells coexpressing streptavidin–KDEL together with GGA1–GFP and CD-MPR (d) or CD-MPR-L274A/L275A (e) reporter proteins were fixed 30 min after the addition of biotin and imaged by Airyscan microscopy. Bar, 2 µm. Arrows indicate carriers containing GGA1–GFP. (f) Airyscan microscopy of HeLa cells coexpressing streptavidin–KDEL together with CD-MPR-L274A/L275A and TfR-Y20A/GDNS$^{31\text{-}34}$AAAA reporter proteins 30 min after the addition of biotin. The inset shows magnified images of the boxed regions. Bars, 1 µm.

microscopy (Polishchuk et al., 2000). These carriers were found to be large (up to 1.7 µm in diameter), tubular-saccular, and devoid of protein coats (Polishchuk et al., 2000), suggestive of their origin in noncoated areas of the Golgi complex. As in our study, they were shown to fuse with the plasma membrane en bloc, without intersecting any other compartment along the way (Hirschberg et al., 1998; Polishchuk et al., 2000). Other immunoelectron studies also demonstrated export of LAMP1 from the TGN in noncoated carriers devoid of cation-independent mannose-6-phosphate receptor and AP-1 but containing VPS41 and VAMP7 (Pols et al., 2013). The latter carriers may correspond to a population that follows the direct pathway and that are less than the level of detection in our assays. Correlative light-electron microscopy of CD-MPR- and GGA1-containing carriers also showed them to be large, convoluted tubular-vesicular structures. However, they have associated clathrin-coated profiles, indicative of their origin at the TGN (Polishchuk et al., 2006). Previous studies showed that, unlike the VSV-G/TfR/LAMP-1 carriers, the CD-MPR/GGA1 carriers did not translocate toward the plasma membrane but merged with endosomes (Puertollano et al., 2003; Waguri et al., 2003; Polishchuk et al., 2006). These properties of the TfR/LAMP1 and CD-MPR carriers are consistent with their being the mediators of transport in the indirect and direct pathways, respectively, to the endolysosomal system. The use of the direct pathway by the CD-MPR fits in with its role as an intracellular sorting receptor for lysosomal hydrolase precursors.

Molecular determinants of early Golgi segregation and Golgi export

Molecular dissection of the endolysosomal proteins used in our study revealed that they have different types of sorting determinant. The initial segregation in the Golgi stack is independent of sorting signals in the cytosolic tails but dependent on the transmembrane and/or luminal domains of the proteins. Transmembrane domains could mediate partitioning into specific lipid domains or interactions with other transmembrane proteins, as shown for other sorting events (Nishikawa and Nakano, 1993; Emery et al., 2003; Alfalah et al., 2005; Patterson et al., 2008; Kaiser et al., 2011). Luminal domains could segregate proteins by promoting oligomerization or aggregation in the special environment of the Golgi complex, as also shown in other settings (Compton et al., 1989; Dintzis et al., 1994; Colomer et al., 1996; Wolins et al., 1997; Paladino et al., 2004). In this regard, it is worth noting that some constitutive secretory cargos, such as the cartilage oligomeric matrix protein and lysozyme C, bind in a Ca^{2+}-dependent manner to the Golgi protein Cab45, which facilitates their export into a specific population of secretory carriers (Crevenna et al., 2016). It is conceivable that a similar mechanism could operate for segregation of transmembrane proteins through their luminal domains. The subsequent packaging of proteins into

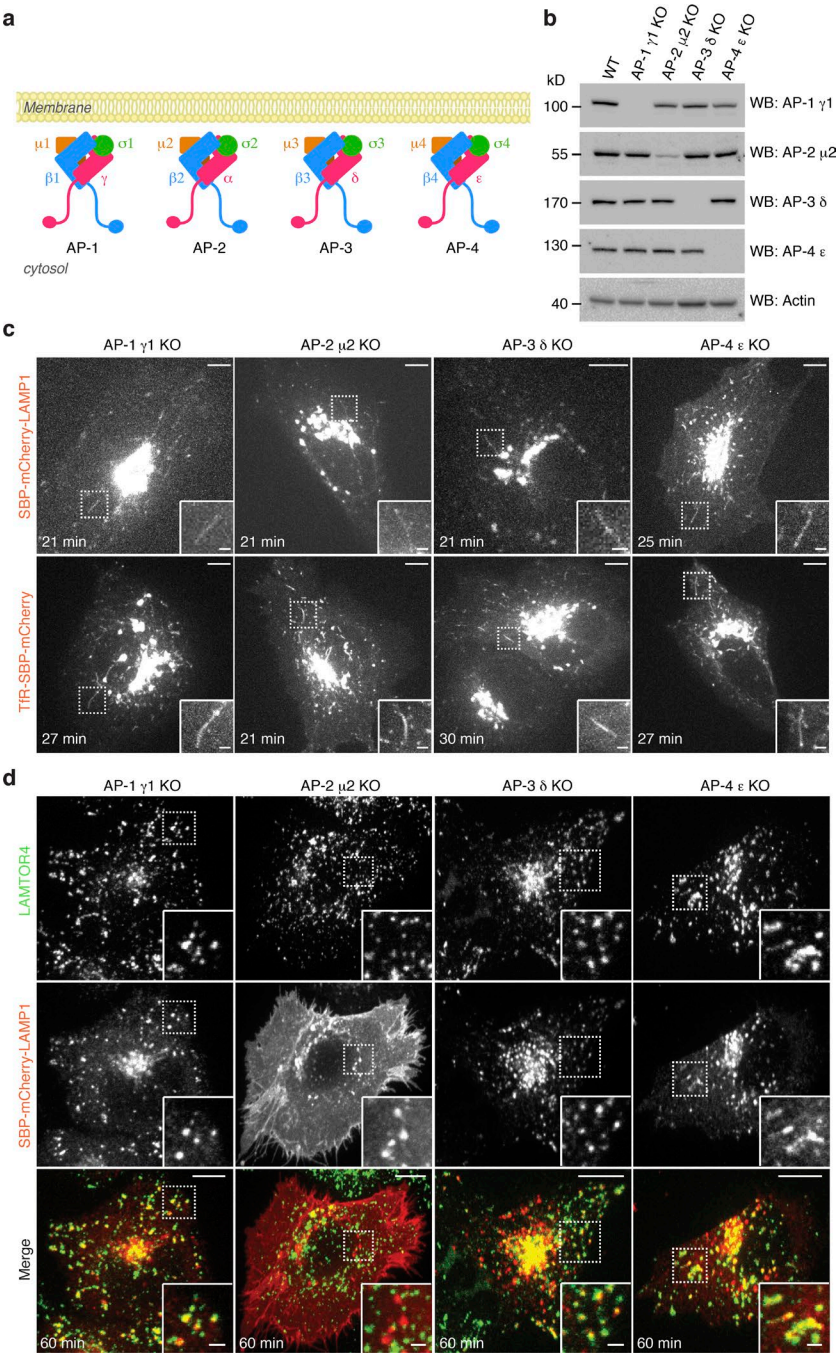

Figure 5. **AP complexes are dispensable for cargo sorting into Golgi-derived tubular carriers.** (a) Schematic representation of AP-1, AP-2, AP-3, and AP-4. (b) Confirmation of KO by immunoblot analysis of endogenous targets. Notice that AP-2 μ2 KO is not complete. Cells with complete KO of AP-2 μ2 were not found in the screening. WB, Western blotting. (c) Images from spinning-disk, live-cell microscopy of LAMP1 or TfR reporter proteins in AP-KO cell lines at the indicated times after biotin addition. Tubular carriers containing LAMP1 or TfR reporters were found in all of the AP-KO cells. Bars: 10 μm; (insets) 1 μm. (d) The LAMP1 reporter protein was expressed in each AP-KO cell line. Cells were fixed 60 min after the addition of biotin and stained for an endogenous lysosomal marker (LAMTOR4) to assess the requirement of AP complexes for transport to lysosomes. Bars: 5 μm; (insets) 1 μm.

Golgi export carriers has long been thought to depend on interactions of cytosolic sorting signals with TGN-associated adaptors such as the GGAs, AP-1, and AP-4. However, for the proteins examined in our study, this appears to be true only for the CD-MPR and sortilin, which require a GGA-binding signal for exit into vesicular carriers. In contrast, exit of TfR and LAMP1 in tubular carriers is independent of sorting signals and of the AP-1, AP-2, AP-3, and AP-4 adaptors. This is in line with the carriers' being the same that transport plasma membrane proteins. AP-2 is subsequently required for endocytosis of TfR and LAMP1 from the plasma membrane, as previously shown by RNAi studies (Motley et al., 2003; Janvier and Bonifacino, 2005). The fact that AP-2 is the only YXXØ-interacting adaptor required for sorting of TfR and LAMP1 to endosomes and lysosomes demonstrates the critical role of endocytosis in this process. Collectively, these observations lend further support to the notion that CD-MPR follows mainly the direct pathway, and TfR and LAMP1 the indirect pathway, for transport to endosomes and lysosomes.

Caveats in the interpretation of our findings

Although the use of the RUSH system has allowed us to track the biosynthetic transport of endolysosomal transmembrane proteins in unprecedented detail, there are several caveats in the interpretation of our experiments. The most important one is that the expression levels of the reporter proteins are likely higher than those of their endogenous counterparts. The mechanics of RUSH could generate a wave of newly synthesized reporter

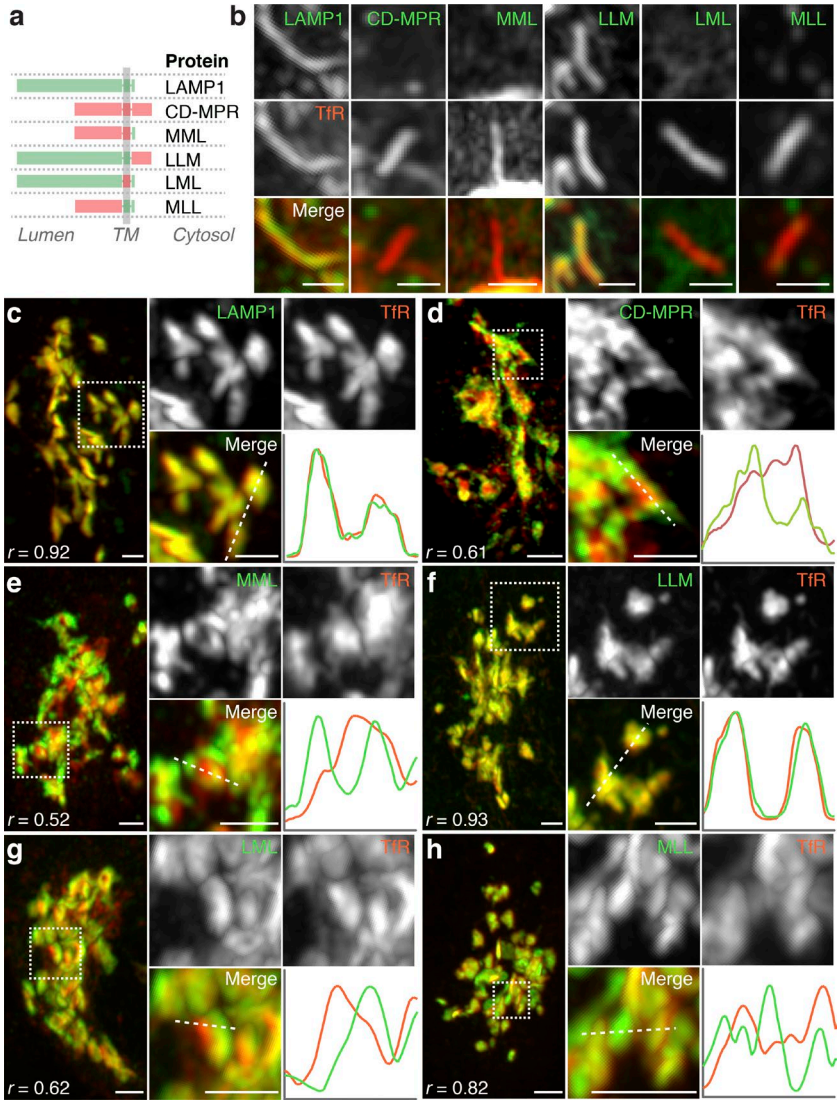

Figure 6. **The luminal and transmembrane domains of endolysosomal proteins determine their intra-Golgi segregation.** (a) Schematic representation of chimeric proteins generated by swapping luminal, transmembrane, and cytosolic domains from LAMP1 (L) and CD-MPR (M). The chimeras were fused to a fluorescent protein and SBP for use as reporter proteins in the RUSH system (Fig. 1 a). (b) HeLa cells coexpressing streptavidin–KDEL together with the indicated chimeras and TfR as reporter proteins were fixed 30 min after the addition of biotin and analyzed by Airyscan microscopy. Bars, 1 µm. Images show the presence or absence of the chimeras in tubular carriers emanating from the Golgi complex. (c–h) Cells in b were similarly imaged for the distribution of the chimeras in the Golgi complex. *r*, Pearson's coefficient. Magnified images and plots of fluorescence intensity along the whited dashed lines are shown at right. Bars, 1 µm.

proteins moving through the secretory pathway, potentially creating abnormal structures or altering the properties of the organelles along the way. Overexpression of the reporter proteins could also saturate sorting dependent on signals and adaptors (Marks et al., 1996). To avoid these problems, in our study we imaged cells expressing moderate levels of the reporter proteins: high enough for detection of transport intermediates but not so high that they changed the appearance of the organelles. In this regard, electron microscopy of cells expressing reporter proteins 25 min after their release from the ER showed normal appearance of the Golgi complex (unpublished data). In addition, saturation of sorting mechanisms would have been expected to homogenize the distribution of different reporters among Golgi domains, transport carriers, and destination organelles, but this was clearly not the case in our studies. These considerations notwithstanding, we cannot rule out the existence of alternative processes, such as populations of CD-MPR following the indirect pathway and TfR and LAMP1 following the direct pathway to some extent.

Hypothetical model for sorting of endolysosomal proteins in the Golgi complex

Our results suggest a two-step process for the sorting of endolysosomal proteins in the Golgi complex (Fig. 7). In the first step, two sets of proteins become segregated to different domains of the Golgi stack by virtue of transmembrane and/or luminal domains. In the second step, proteins segregated to one domain (e.g., CD-MPR) exit the Golgi complex in vesicular carriers bound for the endolysosomal system, in a process that is dependent on recognition of cytosolic sorting signals by clathrin adaptors (i.e., the GGAs). Proteins in the other domain, in contrast, leave the Golgi complex in tubular carriers directed to the plasma membrane, independently of sorting signals and clathrin adaptors. This model differs from the classical model in that different sets of endolysosomal proteins are presorted in the early Golgi and that some of those proteins leave the Golgi complex independently of signal–adaptor interactions.

Materials and methods

Recombinant DNAs

Plasmid constructs to synchronize the traffic of the TfR, LAMP1, CD-MPR, VSV-G, sortilin, and LAMP1–CD-MPR chimeric reporter proteins (Figs. 1 a, 4 a, and 6 a) through the secretory pathway were generated by replacing sequences encoding the reporter proteins in the original bicistronic RUSH constructs (gift of F. Perez

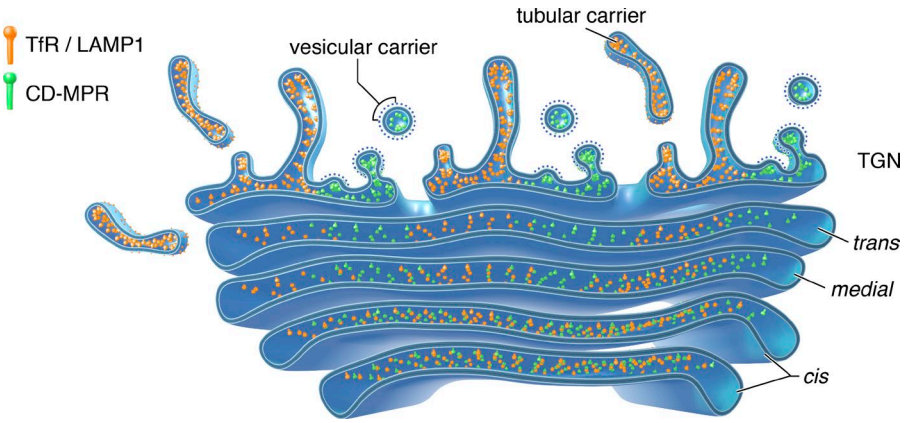

Figure 7. **Model depicting the sorting of endolysosomal proteins in the Golgi complex.** Endolysosomal proteins are delivered from the ER to the Golgi complex in the same transport carriers. Once in the Golgi complex, sets of endolysosomal proteins segregate to distinct domains. One domain gives rise to tubular carriers in which endolysosomal and plasma membrane proteins leave the Golgi independently of cytosolic sorting signals and AP complexes. The other domain is the source of vesicular carriers into which endolysosomal proteins are sorted through interaction of cytosolic sorting signals with GGA proteins.

and G. Boncompain, Curie Institute, Paris, France; Boncompain et al., 2012) in which streptavidin KDEL was used as the hook. The type I transmembrane proteins LAMP1 (UniProt accession no. P14562), CD-MPR (UniProt accession no. P20645), sortilin (UniProt accession no. Q99523), and VSV-G (UniProt accession no. P04882) were modified by insertion of the SBP and a fluorescent protein (EGFP or mCherry) at their luminal N termini, immediately after the signal peptide. The type II transmembrane protein TfR (UniProt accession no. P02786) was tagged with SBP and a fluorescent protein at its luminal C terminus. Tagging in the luminal domain avoided potential interference with cytosolic sorting signals. TfR-Y20A/GDNS31-34AAAA, LAMP1-Y404A, and CD-MPR-L274A/L275A mutants were generated using the QuickChange Site-Directed Mutagenesis kit (Agilent Technologies). Chimeras combining LAMP1 and CD-MPR domains (Fig. 6 a) were generated in the bicistronic RUSH construct using Gibson assembly. LAMP1: luminal, amino acids 22–371; transmembrane, amino acids 372–395; cytosolic, amino acids 396–407. CD-MPR: luminal, amino acids 27–185; transmembrane, amino acids 186–210; cytosolic, amino acids 211–277. EGFP-tagged Rab4a and GGA1 were described previously (Puertollano et al., 2001; Chen et al., 2012).

Antibodies

Mouse monoclonal antibodies to AP-1 γ (1:5,000 for immunoblotting, anti–Adaptin γ; catalog no. 610385), AP-2 µ2 (1:5,000 for immunoblotting, anti-AP50; catalog no. 611351), AP-3 δ (1:5,000 for immunoblotting, anti–Adaptin δ; catalog no. 611329), AP-4 ε (1:5,000 for immunoblotting, anti–Adaptin ε; catalog no. 612018), and actin (1:5,000 for Western blotting, anti-actin; catalog no. 612657) were purchased from BD Biosciences. HRP-conjugated goat anti–mouse antibody (1:5,000 for immunoblotting; catalog no. sc-2004) was purchased from Santa Cruz Biotechnology. Mouse monoclonal antibody to cation-independent mannose-6-phosphate receptor (1:100 for immunofluorescence microscopy, MEM-238; ab8093) was purchased from Abcam. Rabbit monoclonal antibody to LAMTOR4 (1:1,000 for immunofluorescence microscopy; catalog no. 13140) was purchased from Cell Signaling Technology. Alexa-conjugated secondary antibodies including Alexa Fluor 488–conjugated donkey anti–rabbit antibody (1:1,000 for immunofluorescence microscopy; catalog no. A21206) and Alexa Fluor 555–conjugated donkey anti–mouse antibody (1:1,000 for immunofluorescence microscopy; catalog no. A31570) antibodies were purchased from Invitrogen.

Transfection and RUSH

For fixed-cell imaging experiments, 40,000 HeLa cells per well were seeded on a 12-well plate containing 18-mm cover glasses (Marienfeld) coated with fibronectin 1 d before transfection. For live-cell imaging experiments, 40,000 HeLa cells per well were seeded on 2-well Nunc Lab-Tek chambers coated with fibronectin 1 d before transfection. Cells were transfected using FuGENE 6 (E2691; Promega). 6 µl FuGENE transfection reagent was diluted into 80 µl Opti-MEM (31985-070; GIBCO BRL), and, separately, 2 µg DNA was diluted into 20 µl Opti-MEM. For cotransfections, DNA plasmids were combined in an equimolar ratio. After 5 min, the DNA and transfection solutions were mixed and incubated for 20 min before being added to the cells. 20 h after transfection with the indicated plasmids, cells were imaged in 37°C prewarmed phenol red–free medium (20163-029; GIBCO BRL), supplemented with 25 mM Hepes. D-biotin (Sigma-Aldrich) at a final concentration of 40 µM was added to the chamber at time 0.

Fluorescence microscopy

Immunofluorescence microscopy was performed as previously described (Schindler et al., 2015). In brief, HeLa cells were fixed for 30 min at RT in 4% PFA, 4% sucrose, 0.1 mM $CaCl_2$, and 1 mM $MgCl_2$ in PBS. Cells were then permeabilized for 10 min at RT with 0.2% saponin in PBS, followed by incubation with the indicated antibodies. Live-cell imaging was conducted with an Eclipse Ti Microscope System (Nikon) equipped with an environmental chamber (temperature controlled at 37°C and CO_2 at 5%) and NIS-Elements AR microscope imaging software. Spinning-disk confocal images were taken with a Plan Apo VC 60× objective (NA 1.40) and a high-speed electron-multiplying charge-coupled device camera (Evolve 512; Photometrics) mounted on the left portal. TIRF microscopic images were taken with an Apo TIRF 100× Oil DIC N2 objective (NA 1.49) and an electron-multiplying charge-coupled device camera (DU-897; Andor) mounted on the right portal. TIRF position was calibrated for each imaging experiment, and the focus was maintained using a Perfect Focus system. Dual-color imaging was done by fast switching of the excitation lasers, and images from green and red channels were aligned automatically. For TIRF imaging of Alexa Fluor 488–conjugated Tf, transfected cells were incubated in DMEM without FBS, with 1% BSA, for 30 min before being incubated for 1 h in Alexa 488–Tf (working concentration 25 µg/ml; T13342; Thermo Fisher Scientific) at 37°C. RUSH was performed under the constant presence of Alexa Fluor 488–Tf after addition of biotin (which doubled the volume of media, effectively halving the concentration of Tf for the duration of the imaging). Superresolution microscopic images were taken using an LSM 880 microscope with Airyscan (Zeiss) and a Plan Apochromat 63× objective (NA 1.40) with the settings recommended by the manufacturer.

CRISPR/Cas9 KO cells

HeLa-KO cell lines were generated using the CRISPR/Cas9 system (Ran et al., 2013). Target gRNA sequences (AP-1 γ1: 5′-TACATACCG ATGTCGGAATG-3′; AP-2 µ2: 5′-CGATGTCATCTCGGTAGACT-3′; AP-3 δ: 5′-CCTTGTGGTTACGGATGCCG-3′; AP-4 ε: 5′-GCAATC

AAGTTAGCCCAACA-3′) were cloned into the px330 CRISPR/Cas9 vector using the restriction enzyme BbsI. CRISPR/Cas9 constructs were transfected into HeLa cells, and cell lines derived from single colonies were validated by immunoblotting to confirm the loss of the target proteins. For AP-2 µ2, small amounts of the target protein were found in the validation screening, perhaps because of the lethality of complete AP-2 µ2 KO. Rapid accumulation of TfR–SBP–mCherry and SBP–mCherry–LAMP1 on the surface of AP-2 µ2 KO cells was considered confirmation of effective abrogation of AP-2 function (Fig. 5 d and Fig. S5 a).

Flow cytometry

HeLa cells were plated onto six-well plates and transfected with plasmids encoding SBP–GFP–CD-MPR or SBP–GFP–LAMP1 using FuGENE 6. 20 h after transfection, cells were incubated with biotin for 0 and 60 min. All further manipulations were on ice or at 4°C. Cells were detached from the plate by incubating with 10 mM EDTA in PBS for 20 min, pipetting up and down every 5 min. Cells were transferred to 1.5-ml microcentrifuge tubes followed by fixation in PBS containing 4% PFA for 20 min. Cells were washed four times by repeated centrifugation (4°C, 500 *g*, 5 min) in PBS to remove residual PFA. Fixed cells were stained with anti-GFP conjugated with Alexa Fluor 647 (565197; BD Biosciences) at a concentration of 2 µg/ml in PBS containing 3% BSA. Cells were filtered using Cell-Strainer-capped 5-ml round-bottom tubes (352235; Corning). A minimum of 50,000 cells per sample was analyzed using an LSRFortessa cell analyzer (BD Biosciences), gating for GFP-positive cells indicative of expression of the transgene. Data were analyzed using FlowJo software. Surface expression of protein was deduced by relative intensity of Alexa Fluor 647.

Quantitative and statistical analyses

All numerical results are reported as the mean ± SEM and represent data from a minimum of three independent experiments. Line plots were performed in ImageJ. For Fig. 3 (g–i), the first observable robust tubulation from the Golgi was considered time 0 to normalize time points. For live-cell imaging, Imaris was used to calculate the Pearson's correlation of the voxels from the whole image in a z-stack. Images were thresholded at 0.05% of total intensity to reduce background. For each sample, at least seven cells were analyzed per sample. Data were normalized to time point minus 15 min in each data set. A two-tailed Student *t* test for unpaired data were used to evaluate single comparisons between different experimental groups using Microsoft Excel.

For the kinetic analysis of RUSH, SBP–mCherry–LAMP1, SBP–GFP–CD-MPR, or TfR–SBP–mCherry was transfected into HeLa cells 1 d before the experiment. The images were taken by spinning-disk microscopy for 60 min with 3-min time intervals. Only cells with a total intensity at time 0 between 0.5×10^7 and 10^7 arbitrary units were selected to be neither overexpressing nor too affected by bleaching across the 60 min. Because of random lateral movement of the microscopy stage, some time course data sets were stabilized with the image stabilizer plugin for ImageJ (http://www.cs.cmu.edu/~kangli/code/Image_Stabilizer.html). The Golgi was masked and intensity measured across the whole time course in that region. The data set from each cell was normalized so the highest value was equal to 1.

Online supplemental material

Fig. S1 and Video 1 show synchronized transport and eventual destinations of RUSH cargos. Videos 2, 3, 4, 7, and 8 show distinct carriers derived from the Golgi complex for RUSH cargos, and Video 9 shows those for TfR mutant. Figs. S2 and S3 and Videos 5 and 6 show direct fusion of TfR-containing carriers with the plasma membrane. Fig. S4 shows control experiments for cargo segregation in the Golgi complex. Fig. S5 shows different routes for cargos to reach endosomes and lysosomes.

Acknowledgments

We thank Frank Perez and Gaelle Boncompain for kindly providing the original RUSH constructs and Michal Jarnik for help with electron microscopy.

This work was funded by the Intramural Program of the National Institute of Child Health and Human Development, National Institutes of Health (grant ZIA HD001607).

The authors declare no competing financial interests.

Author contributions: Y. Chen and J.S. Bonifacino conceived the project. Y. Chen, D.C. Gershlick, and S.Y. Park performed experiments and analyzed the data. All authors participated in the preparation of the figures and the writing of the manuscript.

Submitted: 31 July 2017
Revised: 18 August 2017
Accepted: 24 August 2017

References

Alfalah, M., G. Wetzel, I. Fischer, R. Busche, E.E. Sterchi, K.P. Zimmer, H.P. Sallmann, and H.Y. Naim. 2005. A novel type of detergent-resistant membranes may contribute to an early protein sorting event in epithelial cells. *J. Biol. Chem.* 280:42636–42643. https://doi.org/10.1074/jbc.M505924200

Ang, A.L., T. Taguchi, S. Francis, H. Fölsch, L.J. Murrells, M. Pypaert, G. Warren, and I. Mellman. 2004. Recycling endosomes can serve as intermediates during transport from the Golgi to the plasma membrane of MDCK cells. *J. Cell Biol.* 167:531–543. https://doi.org/10.1083/jcb.200408165

Boncompain, G., S. Divoux, N. Gareil, H. de Forges, A. Lescure, L. Latreche, V. Mercanti, F. Jollivet, G. Raposo, and F. Perez. 2012. Synchronization of secretory protein traffic in populations of cells. *Nat. Methods.* 9:493–498. https://doi.org/10.1038/nmeth.1928

Bonifacino, J.S., and L.M. Traub. 2003. Signals for sorting of transmembrane proteins to endosomes and lysosomes. *Annu. Rev. Biochem.* 72:395–447. https://doi.org/10.1146/annurev.biochem.72.121801.161800

Braulke, T., and J.S. Bonifacino. 2009. Sorting of lysosomal proteins. *Biochim. Biophys. Acta.* 1793:605–614. https://doi.org/10.1016/j.bbamcr.2008.10.016

Braun, M., A. Waheed, and K. von Figura. 1989. Lysosomal acid phosphatase is transported to lysosomes via the cell surface. *EMBO J.* 8:3633–3640.

Chen, Y., Y. Wang, J. Zhang, Y. Deng, L. Jiang, E. Song, X.S. Wu, J.A. Hammer, T. Xu, and J. Lippincott-Schwartz. 2012. Rab10 and myosin-Va mediate insulin-stimulated GLUT4 storage vesicle translocation in adipocytes. *J. Cell Biol.* 198:545–560. https://doi.org/10.1083/jcb.201111091

Clermont, Y., A. Rambourg, and L. Hermo. 1992. Segregation of secretory material in all elements of the Golgi apparatus in principal epithelial cells of the rat seminal vesicle. *Anat. Rec.* 232:349–358. https://doi.org/10.1002/ar.1092320304

Colomer, V., G.A. Kicska, and M.J. Rindler. 1996. Secretory granule content proteins and the luminal domains of granule membrane proteins aggregate in vitro at mildly acidic pH. *J. Biol. Chem.* 271:48–55. https://doi.org/10.1074/jbc.271.1.48

Compton, T., I.E. Ivanov, T. Gottlieb, M. Rindler, M. Adesnik, and D.D. Sabatini. 1989. A sorting signal for the basolateral delivery of the vesicular stomatitis virus (VSV) G protein lies in its luminal domain: analysis of the targeting of VSV G-influenza hemagglutinin chimeras. *Proc. Natl. Acad. Sci. USA.* 86:4112–4116. https://doi.org/10.1073/pnas.86.11.4112

Crevenna, A.H., B. Blank, A. Maiser, D. Emin, J. Prescher, G. Beck, C. Kienzle, K. Bartnik, B. Habermann, M. Pakdel, et al. 2016. Secretory cargo sorting by Ca2+-dependent Cab45 oligomerization at the trans-Golgi network. *J. Cell Biol.* 213:305–314. https://doi.org/10.1083/jcb.201601089

Dintzis, S.M., V.E. Velculescu, and S.R. Pfeffer. 1994. Receptor extracellular domains may contain trafficking information. Studies of the 300-kDa mannose 6-phosphate receptor. *J. Biol. Chem.* 269:12159–12166.

Emery, G., R.G. Parton, M. Rojo, and J. Gruenberg. 2003. The trans-membrane protein p25 forms highly specialized domains that regulate membrane composition and dynamics. *J. Cell Sci.* 116:4821–4832. https://doi.org/10.1242/jcs.00802

Gravotta, D., J.M. Carvajal-Gonzalez, R. Mattera, S. Deborde, J.R. Banfelder, J.S. Bonifacino, and E. Rodriguez-Boulan. 2012. The clathrin adaptor AP-1A mediates basolateral polarity. *Dev. Cell.* 22:811–823. https://doi.org/10.1016/j.devcel.2012.02.004

Griffiths, G., and K. Simons. 1986. The trans Golgi network: sorting at the exit site of the Golgi complex. *Science.* 234:438–443. https://doi.org/10.1126/science.2945253

Harter, C., and I. Mellman. 1992. Transport of the lysosomal membrane glycoprotein lgp120 (lgp-A) to lysosomes does not require appearance on the plasma membrane. *J. Cell Biol.* 117:311–325. https://doi.org/10.1083/jcb.117.2.311

Hirschberg, K., C.M. Miller, J. Ellenberg, J.F. Presley, E.D. Siggia, R.D. Phair, and J. Lippincott-Schwartz. 1998. Kinetic analysis of secretory protein traffic and characterization of Golgi to plasma membrane transport intermediates in living cells. *J. Cell Biol.* 143:1485–1503. https://doi.org/10.1083/jcb.143.6.1485

Janvier, K., and J.S. Bonifacino. 2005. Role of the endocytic machinery in the sorting of lysosome-associated membrane proteins. *Mol. Biol. Cell.* 16:4231–4242. https://doi.org/10.1091/mbc.E05-03-0213

Kaiser, H.J., A. Orłowski, T. Róg, T.K. Nyholm, W. Chai, T. Feizi, D. Lingwood, I. Vattulainen, and K. Simons. 2011. Lateral sorting in model membranes by cholesterol-mediated hydrophobic matching. *Proc. Natl. Acad. Sci. USA.* 108:16628–16633. https://doi.org/10.1073/pnas.1103742108

Klumperman, J., A. Hille, T. Veenendaal, V. Oorschot, W. Stoorvogel, K. von Figura, and H.J. Geuze. 1993. Differences in the endosomal distributions of the two mannose 6-phosphate receptors. *J. Cell Biol.* 121:997–1010. https://doi.org/10.1083/jcb.121.5.997

Ladinsky, M.S., J.R. Kremer, P.S. Furcinitti, J.R. McIntosh, and K.E. Howell. 1994. HVEM tomography of the trans-Golgi network: structural insights and identification of a lace-like vesicle coat. *J. Cell Biol.* 127:29–38. https://doi.org/10.1083/jcb.127.1.29

Lippincott-Schwartz, J., and D.M. Fambrough. 1986. Lysosomal membrane dynamics: Structure and interorganellar movement of a major lysosomal membrane glycoprotein. *J. Cell Biol.* 102:1593–1605. https://doi.org/10.1083/jcb.102.5.1593

Marks, M.S., L. Woodruff, H. Ohno, and J.S. Bonifacino. 1996. Protein targeting by tyrosine- and di-leucine-based signals: Evidence for distinct saturable components. *J. Cell Biol.* 135:341–354. https://doi.org/10.1083/jcb.135.2.341

Micaroni, M., A.C. Stanley, T. Khromykh, J. Venturato, C.X. Wong, J.P. Lim, B.J. Marsh, B. Storrie, P.A. Gleeson, and J.L. Stow. 2013. Rab6a/a′ are important Golgi regulators of pro-inflammatory TNF secretion in macrophages. *PLoS One.* 8:e57034. https://doi.org/10.1371/journal.pone.0057034

Motley, A., N.A. Bright, M.N. Seaman, and M.S. Robinson. 2003. Clathrin-mediated endocytosis in AP-2-depleted cells. *J. Cell Biol.* 162:909–918. https://doi.org/10.1083/jcb.200305145

Munro, S., and H.R. Pelham. 1987. A C-terminal signal prevents secretion of luminal ER proteins. *Cell.* 48:899–907. https://doi.org/10.1016/0092-8674(87)90086-9

Nielsen, M.S., P. Madsen, E.I. Christensen, A. Nykjaer, J. Gliemann, D. Kasper, R. Pohlmann, and C.M. Petersen. 2001. The sortilin cytoplasmic tail conveys Golgi-endosome transport and binds the VHS domain of the GGA2 sorting protein. *EMBO J.* 20:2180–2190. https://doi.org/10.1093/emboj/20.9.2180

Nishikawa, S., and A. Nakano. 1993. Identification of a gene required for membrane protein retention in the early secretory pathway. *Proc. Natl. Acad. Sci. USA.* 90:8179–8183. https://doi.org/10.1073/pnas.90.17.8179

Odorizzi, G., and I.S. Trowbridge. 1997. Structural requirements for basolateral sorting of the human transferrin receptor in the biosynthetic and endocytic pathways of Madin-Darby canine kidney cells. *J. Cell Biol.* 137:1255–1264. https://doi.org/10.1083/jcb.137.6.1255

Paladino, S., D. Sarnataro, R. Pillich, S. Tivodar, L. Nitsch, and C. Zurzolo. 2004. Protein oligomerization modulates raft partitioning and apical sorting of GPI-anchored proteins. *J. Cell Biol.* 167:699–709. https://doi.org/10.1083/jcb.200407094

Patterson, G.H., K. Hirschberg, R.S. Polishchuk, D. Gerlich, R.D. Phair, and J. Lippincott-Schwartz. 2008. Transport through the Golgi apparatus by rapid partitioning within a two-phase membrane system. *Cell.* 133:1055–1067. https://doi.org/10.1016/j.cell.2008.04.044

Polishchuk, E.V., A. Di Pentima, A. Luini, and R.S. Polishchuk. 2003. Mechanism of constitutive export from the golgi: bulk flow via the formation, protrusion, and en bloc cleavage of large trans-Golgi network tubular domains. *Mol. Biol. Cell.* 14:4470–4485. https://doi.org/10.1091/mbc.E03-01-0033

Polishchuk, R.S., E.V. Polishchuk, P. Marra, S. Alberti, R. Buccione, A. Luini, and A.A. Mironov. 2000. Correlative light-electron microscopy reveals the tubular-saccular ultrastructure of carriers operating between Golgi apparatus and plasma membrane. *J. Cell Biol.* 148:45–58. https://doi.org/10.1083/jcb.148.1.45

Polishchuk, R.S., E. San Pietro, A. Di Pentima, S. Teté, and J.S. Bonifacino. 2006. Ultrastructure of long-range transport carriers moving from the trans Golgi network to peripheral endosomes. *Traffic.* 7:1092–1103. https://doi.org/10.1111/j.1600-0854.2006.00453.x

Pols, M.S., E. van Meel, V. Oorschot, C. ten Brink, M. Fukuda, M.G. Swetha, S. Mayor, and J. Klumperman. 2013. hVps41 and VAMP7 function in direct TGN to late endosome transport of lysosomal membrane proteins. *Nat. Commun.* 4:1361. https://doi.org/10.1038/ncomms2360

Puertollano, R., R.C. Aguilar, I. Gorshkova, R.J. Crouch, and J.S. Bonifacino. 2001. Sorting of mannose 6-phosphate receptors mediated by the GGAs. *Science.* 292:1712–1716. https://doi.org/10.1126/science.1060750

Puertollano, R., N.N. van der Wel, L.E. Greene, E. Eisenberg, P.J. Peters, and J.S. Bonifacino. 2003. Morphology and dynamics of clathrin/GGA1-coated carriers budding from the trans-Golgi network. *Mol. Biol. Cell.* 14:1545–1557. https://doi.org/10.1091/mbc.02-07-0109

Puthenveedu, M.A., C. Bachert, S. Puri, F. Lanni, and A.D. Linstedt. 2006. GM130 and GRASP65-dependent lateral cisternal fusion allows uniform Golgi-enzyme distribution. *Nat. Cell Biol.* 8:238–248. https://doi.org/10.1038/ncb1366

Ran, F.A., P.D. Hsu, J. Wright, V. Agarwala, D.A. Scott, and F. Zhang. 2013. Genome engineering using the CRISPR-Cas9 system. *Nat. Protoc.* 8:2281–2308. https://doi.org/10.1038/nprot.2013.143

Robinson, M.S. 2004. Adaptable adaptors for coated vesicles. *Trends Cell Biol.* 14:167–174. https://doi.org/10.1016/j.tcb.2004.02.002

Schindler, C., Y. Chen, J. Pu, X. Guo, and J.S. Bonifacino. 2015. EARP is a multisubunit tethering complex involved in endocytic recycling. *Nat. Cell Biol.* 17:639–650. https://doi.org/10.1038/ncb3129

Tie, H.C., D. Mahajan, B. Chen, L. Cheng, A.M. VanDongen, and L. Lu. 2016. A novel imaging method for quantitative Golgi localization reveals differential intra-Golgi trafficking of secretory cargoes. *Mol. Biol. Cell.* 27:848–861. https://doi.org/10.1091/mbc.E15-09-0664

Traub, L.M., and J.S. Bonifacino. 2013. Cargo recognition in clathrin-mediated endocytosis. *Cold Spring Harb. Perspect. Biol.* 5:a016790. https://doi.org/10.1101/cshperspect.a016790

Tveit, H., G. Dick, V. Skibeli, and K. Prydz. 2005. A proteoglycan undergoes different modifications en route to the apical and basolateral surfaces of Madin-Darby canine kidney cells. *J. Biol. Chem.* 280:29596–29603. https://doi.org/10.1074/jbc.M503691200

Vuong, T.T., K. Prydz, and H. Tveit. 2006. Differences in the apical and basolateral pathways for glycosaminoglycan biosynthesis in Madin-Darby canine kidney cells. *Glycobiology.* 16:326–332. https://doi.org/10.1093/glycob/cwj075

Waguri, S., F. Dewitte, R. Le Borgne, Y. Rouillé, Y. Uchiyama, J.F. Dubremetz, and B. Hoflack. 2003. Visualization of TGN to endosome trafficking through fluorescently labeled MPR and AP-1 in living cells. *Mol. Biol. Cell.* 14:142–155. https://doi.org/10.1091/mbc.E02-06-0338

Wolins, N., H. Bosshart, H. Küster, and J.S. Bonifacino. 1997. Aggregation as a determinant of protein fate in post-Golgi compartments: Role of the luminal domain of furin in lysosomal targeting. *J. Cell Biol.* 139:1735–1745. https://doi.org/10.1083/jcb.139.7.1735

Yano, H., M. Yamamoto-Hino, M. Abe, R. Kuwahara, S. Haraguchi, I. Kusaka, W. Awano, A. Kinoshita-Toyoda, H. Toyoda, and S. Goto. 2005. Distinct functional units of the Golgi complex in *Drosophila* cells. *Proc. Natl. Acad. Sci. USA.* 102:13467–13472. https://doi.org/10.1073/pnas.0506681102

Zhu, Y., B. Doray, A. Poussu, V.P. Lehto, and S. Kornfeld. 2001. Binding of GGA2 to the lysosomal enzyme sorting motif of the mannose 6-phosphate receptor. *Science.* 292:1716–1718. https://doi.org/10.1126/science.1060896